Damage Deactivation of Engineering Materials and Structures

Artur Ganczarski and Marcin Cegielski

Abstract When a material is subjected to a cyclic loading at high values of stress or strain, damage develops together with cyclic plastic strain. This process is often accompanied by damage deactivation characterized by actual state of microcracks, which are generally active under tension and passive under compression. In classical formulation damage deactivation occurs instantly when loading changes sign and consequently leads to non smooth path separating both load ranges. The real materials, however, do not exhibit such bilinear paths. Therefore, the more realistic model based on continuous damage deactivation is proposed, in which microcracks close gradually. In the present paper several applications of continuous damage deactivation in modelling of cycle fatigue of engineering materials such as: aluminum alloy Al-2024 and ferritic steel 20MnMoNi55 are demonstrated and compared with experimental results. Detail quantitative and qualitative analysis of obtained solutions confirms necessity and correctness of proposed approach.

1 Introduction

In the case of cycle fatigue, when the stress level is larger than the yield stress, damage develops together with the cyclic plastic strain, after the incubation period that precedes the nucleation and growth of micro-defects is met. In the most frequent approach to the cycle fatigue, in case when a loading is the periodic strain-controlled of constant amplitude, the following assumptions are made: the material becomes perfectly plastic during first cycle, the variation of damage is neglected for

A. Ganczarski (✉) · M. Cegielski
Institute of Applied Mechanics, Cracow University of Technology,
Al. Jana Pawła II 37, 31-864 Kraków, Poland
e-mail: artur@cut1.mech.pk.edu.pl

M. Cegielski
e-mail: morf1@o2.pl

H. Altenbach and S. Kruch (eds.), *Advanced Materials Modelling for Structures*,
Advanced Structured Materials 19, DOI: 10.1007/978-3-642-35167-9_15,

the integration over one cycle and the strain-damage relations are identical both for tension and compression. These allow to simplify calculations of damage cumulation per one cycle and give linear dependency of damage with number of cycles, finally leading to the Manson-Coffin law of low cycle fatigue [18, 23].

On the other hand, the more refined approaches to cycle fatigue [2, 17], based on the kinetic theory of damage evolution and the Gurson-Tvergaard-Needleman model of damage incorporating isotropic hardening, respectively, are able to predict some qualitative phenomena of damage accumulation, crack initiation and fracture only approximately, since they do not account for the unilateral damage.

The phenomenon of the unilateral damage, also called the damage deactivation or the crack closure/opening effect is typical for materials subjected to reverse tension-compression cycles. In the simplest one-dimensional case, if the loading is reversed from tension to compression, the cracks will completely close such that the material behaves as uncracked, or in other words, its initial stiffness is recovered. The mathematical description of unilateral damage is based on the decomposition of the stress or strain into the positive and negative projections [14, 16, 19, 20]. In the simplest case the damage modified stress or strain are used, based on the concept of the Heaviside function, where the negative principal components are ruled out. This means that the negative principal strain or stress components become completely inactive in further damage process as long as the loading condition can again render them active [19]. In a more general approach, both positive and weighted negative eigenvalues of strain or stress tensors influence damage evolution [12, 21]. The positive parts of the strain or stress can also be expressed by the use of the fourth-order positive projection operators written in terms of their eigenvectors [11, 14]. The limitations of the consistent unilateral damage condition applied to the continuum damage theories have been discussed in [4–6]. Authors showed that in the existing theories developed in [13, 15, 22] either non-symmetries of the elastic stiffness or non-realistic discontinuities of the stress-strain response may occur for general multiaxial non-proportional loading conditions. It is easy to show that if the unilateral condition does affect both the diagonal and the off-diagonal terms of the stiffness or compliance tensor, a stress discontinuity takes place when one of principal strains changes sign and the other remain unchanged [24]. In the model proposed in [5] only the diagonal components corresponding to negative normal strains are replaced by the initial (undamaged) values. The consistent description of the unilateral effect was recently developed in [9, 10]. Authors introduced a new fourth-rank damage parameter built upon the eigenvectors of second-order damage tensor that controls the crack closure effect with the continuity requirement of the stress-strain response fulfilled.

2 Concept of Continuous Damage Deactivation

In case of uniaxial state of stress and scalar damage, micro-cracks remain open under tension and almost entirely close under compression, hence the effective stress and the appropriate effective modulus of elasticity are defined in [17] as follows

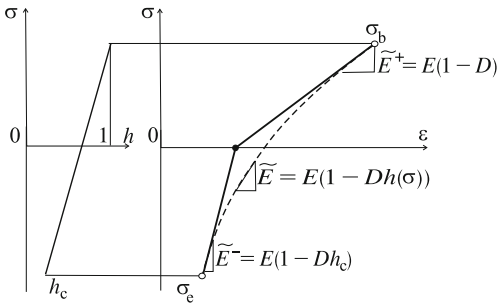

Fig. 1 Concept of the continuous damage deactivation

$$\widetilde{\sigma} = \begin{cases} \sigma/(1-D) \\ \sigma/(1-Dh) \end{cases} \qquad \widetilde{E} = \begin{cases} E\,(1-D) & \text{if} \quad \sigma > 0 \\ E\,(1-Dh) & \text{if} \quad \sigma < 0 \end{cases} \tag{1}$$

Above formulas contain the crack closure parameter h $(0 \leq h \leq 1)$, that depends on a material and loading, however, in practice it is considered to be constant $h = h_c = 0.2$. Application of this model for description of unloading path leads to linear relation between the stress decrease and the strain decrease given by $\widetilde{E}^{+}$. Entering the compression range the material switches to the path characterized by the modulus of elasticity which is equal to $\widetilde{E}^{-}$ (solid line in Fig. 1). The real materials do not exhibit such bilinear unloading paths, therefore the concept of continuous crack closure that allows to eliminate mentioned switch between $\widetilde{E}^{+}$ and $\widetilde{E}^{-}$ is introduced. It consists in the replacement of parameter h by a function $h(\sigma)$, being linear in the simplest case, such that

$$h\,(\sigma) = h_c + (1-h_c)\,(\sigma - \sigma_e)/(\sigma_b - \sigma_e) \tag{2}$$

According to above relation function $h(\sigma)$ is equal to 1 when $\sigma = \sigma_b$ and h_c when $\sigma = \sigma_e$, see Fig. 1.

Three-dimensional generalization of the continuous damage deactivation requires distinction between tension and compression. When the stress tensor is given by its eigenvalues the following decomposition proposed in [17] is applied

$$\boldsymbol{\sigma} = \text{diag}\,\{\sigma_1, \sigma_2, \sigma_3\} = \langle \boldsymbol{\sigma} \rangle - \langle -\boldsymbol{\sigma} \rangle \tag{3}$$

In case of isotropic damage and application of the principle of strain equivalence the general form of effective stress proposed in [17] is as follows

$$\widetilde{\boldsymbol{\sigma}} = \pm \frac{\langle \pm \boldsymbol{\sigma} \rangle}{1-Dh} \pm \frac{\nu}{1-2\nu} \frac{[\text{Tr}\,\langle \pm \boldsymbol{\sigma} \rangle - \langle \pm \text{Tr}(\boldsymbol{\sigma}) \rangle]\mathbf{1}}{(1-Dh)} \tag{4}$$

Terms associated to the factor $\nu/(1-2\nu)$, introducing coupling, disappear if all eigenvalues of stress are of the same sign and in such case simplified effective stresses and the corresponding elastic modules take the form

$$\widetilde{\boldsymbol{\sigma}} = \begin{cases} \langle \boldsymbol{\sigma} \rangle / (1 - D) \\ -\langle -\boldsymbol{\sigma} \rangle / (1 - Dh) \end{cases} \qquad \widetilde{\mathbf{E}} = \begin{cases} \mathbf{E}(1 - D) & \text{“tension”} \\ \mathbf{E}(1 - Dh) & \text{“compression”} \end{cases} \tag{5}$$

Application of the concept of continuous crack closure needs additional hypothesis that introduces the relation between the crack closure magnitude and a scalar function of the stress tensor

$$h(\boldsymbol{\sigma}) = h_{\mathrm{c}} + (1 - h_{\mathrm{c}})[\chi(\boldsymbol{\sigma}) - \chi(\boldsymbol{\sigma}_{\mathrm{e}})]/[\chi(\boldsymbol{\sigma}_{\mathrm{b}}) - \chi(\boldsymbol{\sigma}_{\mathrm{e}})] \tag{6}$$

here the known Hayhurst function

$$\chi(\boldsymbol{\sigma}) = \beta \mathrm{Tr}(\boldsymbol{\sigma}) + (1 - \beta) J_2(\boldsymbol{\sigma}) \tag{7}$$

3 Examples

3.1 Low Cycle Fatigue of Aluminum Alloy Al-2024

The objective of this example is the modelling of damage deactivation concept in the aluminum alloy Al-2024 in order to describe the phenomenon of non-symmetric hysteresis loop evolution due to different damage growth under tension and compression observed in experiment [1], see Fig. 2a. Detailed analysis of the subsequent strain-stress loops, obtained in uniaxial tension-compression test at the constant strain amplitude $\Delta\varepsilon = \pm 1\,\%$, confirms an elasto-plastic behavior of the material and strong influence of the unilateral damage effect. During the initial cycles the material exhibits plastic hardening leading to the stabilized cycle and, then asymmetric drop

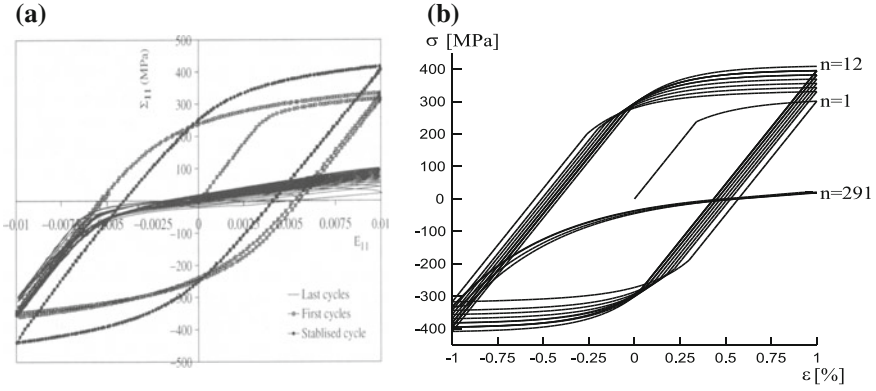

Fig. 2 Cycle fatigue for aluminum alloy Al-2024: **a** tension-compression test [1], **b** numerical simulation with model of continuous damage deactivation [8]

of both the stress amplitude and the modulus of elasticity reveals following damage growth. This process is accompanied by a gradual decrease of the hysteresis area and a change of shape of subsequent hysteresis loops, associated with a formation of the characteristic inflection point on their lower branches. Description of plastic flow including degradation of material properties by damage, able to model experiment is based on the kinetic of damage evolution [17, 18]. In case of uniaxial stress state the dissipation potential being a sum of the plastic and damage potentials is assumed in simplified form

$$F = |\widetilde{\sigma} - X| - R - \sigma_{\mathrm{y}} + 0.75X^2/X_{\infty} + Y^2 H(p - p^{\mathrm{D}})/2S(1 - Dh) \quad (8)$$

where elastic strain energy density release rate is equal to $Y = \widetilde{\sigma}^2/2E$. Application of the formalism of associated plasticity leads to the following evolution equations [8]

$$\begin{aligned}
&\mathrm{d}\sigma/\mathrm{d}\varepsilon = E\,(1 - Dh) && \text{elastic range}\\
&\mathrm{d}\sigma/\mathrm{d}p = (1 - Dh)^2 \left\{\left[X_{\infty}\gamma + b\,(R_{\infty} - R)\right]\mathrm{sgn}\,(\widetilde{\sigma} - X) - \gamma X\right\} && \text{plastic range}\\
&\qquad\qquad -\widetilde{\sigma}^3 H(p - p^{\mathrm{D}})/2ES\\
&\mathrm{d}R/\mathrm{d}p = b\,(R_{\infty} - R)\,(1 - Dh)\\
&\mathrm{d}X/\mathrm{d}p = \gamma\left[X_{\infty}\mathrm{sgn}\,(\mathrm{d}\varepsilon^{\mathrm{p}}) - X\right](1 - Dh)\\
&\mathrm{d}D/\mathrm{d}p = \sigma^2 H\left(p - p^{\mathrm{D}}\right)/2ES\,(1 - Dh)^2
\end{aligned} \quad (9)$$

The effect of continuous damage deactivation describe by Eq. (2) is limited by the additional assumption that the stress referring to the beginning of damage deactivation is equal to $\sigma_{\mathrm{b}} = 0$. Magnitudes of all material constants defining model are given in Table 1. Numerical integration of system of evolution equations (9) for constant strain range $\Delta\varepsilon = \pm 1\,\%$ is done by use of the fourth-order Runge-Kutta technique with the adaptive stepsize control. Model under consideration properly maps unilateral nature of damage softening, in this sense that the dead center ordinates of subsequent hysteresis loops coincide exactly with the appropriate points on experimental curves, see Fig. 2b. Additionally, a gradually decreasing area of the subsequent hysteresis loops and accompanying change of curvature at their unloading branch, are well mapped.

Table 1 Material data for alloy Al-2024

E [GPa]	σ_{y} [MPa]	b	R_{∞} [MPa]	γ	X_{∞} [MPa]	S [MPa]	p^{D}
70	230	0.1	120	4.0	60	3500	0.248

3.2 Yield Surface Affected by Damage

Damage evolution equations presented in the previous example are derived on the basis of kinetic law of damage evolution [17, 18]. Key point of this theory is the

potential of dissipation taken as a sum of the plastic potential referring to theory of associated plasticity and a damage dissipation potential. In the simplest case of isotropic damage and absence of both kinematic and isotropic hardening, it is assumed that the kinetic coupling acts only by the effective stress deviator and this corresponds to the following yield function

$$f(\boldsymbol{\sigma}, Dh) = 0 \tag{10}$$

Simultaneously, it is postulated that the yield function f is a scalar continuous or partly continuous (having at most finite set of corner points) and convex function. Form of yield function is strictly associated with magnitude of damage deactivation parameter h in Eq. (10) and consequently essentially differs in case of tension when damage is active than in case of compression when damage remains inactive. In case of the plane stress state and under assumption that damage is active if only one of stress components is positive ($\sigma_1 > 0$ or $\sigma_2 > 0$) or in other words $h = 1$ if $\mathrm{Tr}\,\langle\boldsymbol{\sigma}\rangle$ is positive, yield potential takes following form

$$\sigma_1^2 - \sigma_1\sigma_2 + \sigma_2^2 = \begin{cases} \sigma_y^2 (1-D)^2 & 1^{\mathrm{st}}, 2^{\mathrm{nd}}, 4^{\mathrm{th}} \text{ quarter} \\ \sigma_y^2 & 3^{\mathrm{rd}} \text{ quarter} \end{cases} \tag{11}$$

and turns out to be non-smooth and non-convex (Fig. 3a). The above mentioned defect of yield potential may be successfully removed by introducing continuous damage deactivation, when micro-cracks do not close instantaneously but gradually Eq. (6). Restricting considerations to the simplified case when $\chi(\boldsymbol{\sigma})$ in Eq. (7) depends only on positive value of the first invariant of stress tensor ($\beta = 1$ and $\mathrm{Tr}(\boldsymbol{\sigma}) = \mathrm{Tr}\,\langle\boldsymbol{\sigma}\rangle$). Assuming further that micro-cracks are fully open under maximum tension $\sigma_b = 2(1-D)\sigma_y/\sqrt{3}$ and close completely under compression ($h_c = 0$) the yield function is given by formulas

$$\sigma_1^2 - \sigma_1\sigma_2 + \sigma_2^2 = \begin{cases} \sigma_y^2 (1-D)^2 & \text{arc } C_1C_2 \\ \sigma_y^2 \left(1 - \frac{D}{1-D}\frac{\sqrt{3}}{2}\frac{\sigma_{2/1}}{\sigma_y}\right)^2 & \text{arcs } C_1A_2 \text{ or } C_2B_2 \\ \sigma_y^2 & \text{arc } A_2B_2 \end{cases} \tag{12}$$

Now yield function is composed of two ellipses and two hyperbolas and its convexity and smoothness are recovered (Fig. 3b). Subsequent stages of damage affected yield function versus experimental investigations (isochronous creep curves) [19] are shown in Fig. 3c, d.

3.3 Low Cycle Fatigue of Notch Specimen Made of Ferritic Steel

Success in modelling of low cycle fatigue of alloy Al-2024 as well as recovery of both convexity and smoothness of yield function allow to consider more advanced

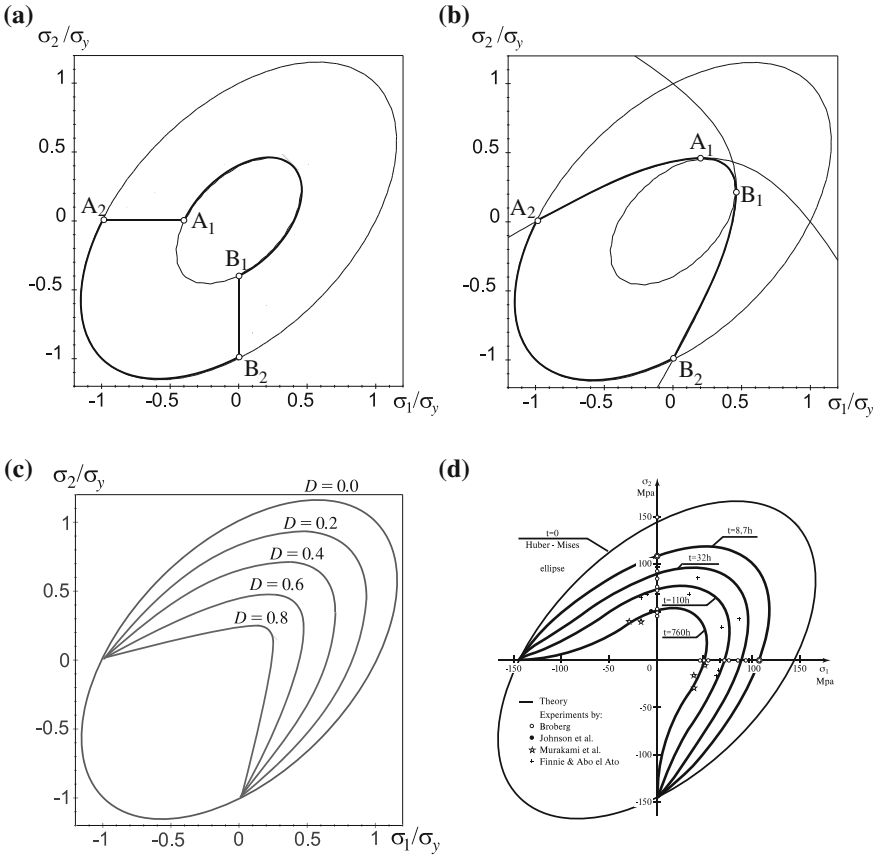

Fig. 3 Yield function affected by damage: **a** non-smooth and non-convex case corresponding to discontinuous damage deactivation ($D = 0.6$), **b** smooth and convex after application of continuous damage deactivation ($D = 0.6$), **c** subsequent yield functions [7], **d** experimental investigations [19]

3D problem. Cyclic test with elongation controlled amplitudes $\Delta l = \pm 0.1$ mm of notched specimens made of ferritic steel 20MnMoNi55 was done in [2]. Subsequent elongation-cyclic load curves, exhibiting Bauschinger-like continuously softening effect are shown in Fig. 4a. A crack initiates at the notch root and extends through the specimen diameter. The test was stopped after 83 cycles to examine the damage evolution.

Analogously to the previous example, inelastic deformation is described in framework of kinetic law of damage evolution [17, 18] generalized for the case of finite deformation. The dissipation potential is assumed in following form

$$F = J_2(\widetilde{\mathbf{S}}' - \mathbf{X}') - R - \sigma_{\mathrm{y}} + 0.75\mathbf{X}' : \mathbf{X}'/X_\infty + F^{\mathrm{D}}(Y, D) \tag{13}$$

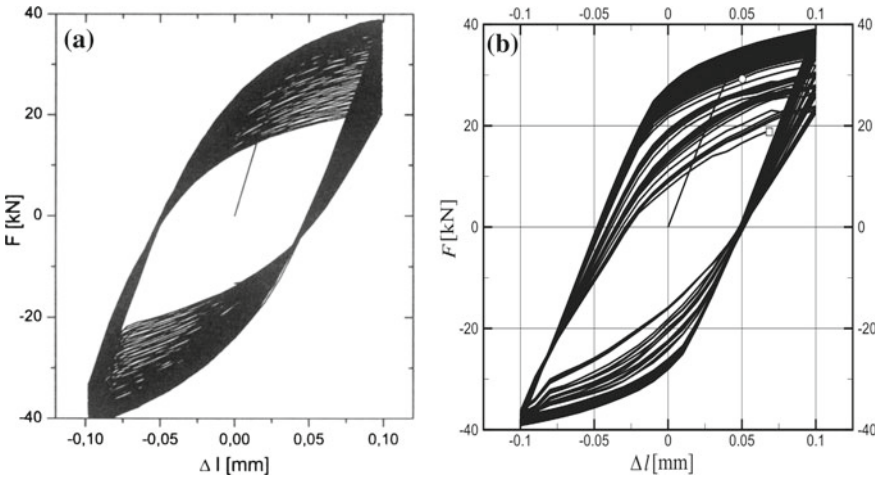

Fig. 4 Cyclic load versus elongation of specimen made of ferritic steel 20MnMoNi55: **a** test result [2], **b** simulation with finite element model [3]

The elastic deformation is described by Hooke's law in which the effective elastic tensor $\widetilde{\mathbf{E}}$ is given by Eq. (5). The associated flow rule defines plastic deformation

$$\mathrm{d}\mathbf{e}^{\mathrm{p}} = 1.5(\widetilde{\mathbf{S}}' - \mathbf{X}')\mathrm{d}\lambda/[J_2(\widetilde{\mathbf{S}}' - \mathbf{X}')(1 - Dh)] \tag{14}$$

whereas the cumulative plastic strain is equal

$$\mathrm{d}p = \sqrt{2\mathrm{d}\mathbf{e}^{\mathrm{p}} : \mathrm{d}\mathbf{e}^{\mathrm{p}}/3} = \mathrm{d}\lambda/(1 - Dh) \tag{15}$$

Application of formalism of associated plasticity yields following evolution equations for isotropic and kinematic hardening

$$\mathrm{d}R/\mathrm{d}\lambda = b(R_\infty - R) \qquad \mathrm{d}\mathbf{X}'/\mathrm{d}\lambda = \gamma[2X_\infty \mathrm{d}\boldsymbol{\varepsilon}^{\mathrm{p}}(1 - Dh)/3\mathrm{d}\lambda - \mathbf{X}'] \tag{16}$$

both dependent on plastic multiplier which is to satisfy the consistency condition

$$\partial F/\partial \mathbf{S}' : \mathrm{d}\mathbf{S}' + \partial F/\partial \mathbf{X}' : \mathrm{d}\mathbf{X}' + \partial F/\partial R : \mathrm{d}R = 0 \tag{17}$$

The strain energy density release rate based on Eq. (13) is equal to

$$Y = 0.5\mathbf{E}^{-1} : \widetilde{\mathbf{S}} : \widetilde{\mathbf{S}} \tag{18}$$

hence damage evolution equation takes the following form

$$\mathrm{d}D/\mathrm{d}p = \mathbf{E}^{-1} : \mathbf{S} : \mathbf{S}\, H(p - p^{\mathrm{D}})/[2S(1 - Dh)^2] \tag{19}$$

Described formalism referring to the total Lagrangian formulation is implemented into finite element code for quadrilateral axisymmetric elements. Magnitudes of material constants, identified by Brocks and Steglich [2], are demonstrated in Table 2. The numerical simulation exhibits all quantitative phenomena of decreasing load due to damage evolution with damage localization starting at the notch root, see Fig. 4b, as in the experiment. Value of damage parameter $D \geq 0.87$ indicates complete loss of stress carrying capacity of the respective element and hence cracking. The number of cycles to failure is equal to about one half when compare to experiment. Further analysis associated with propagation of damage front inside the material is possible if one of special techniques, referring to numerical solution of singular boundary value problem, is applied. Application of classical methods based on Gaussian elimination or LU decomposition is possible as long as system of equations or global stiffness matrix remain nonsingular in mathematical or numerical sense. In other words, this means that critical magnitude of damage $D = 1.0$ is attainable only with certain tolerance since appropriate effective stress Eq. (5) approaches infinity whereas effective stiffness Eq. (5) tends to zero. In all such cases, when global stiffness matrix becomes singular the special techniques of FEM, based on turning off completely damaged elements or substituting by elements of zero or negligible stiffness, turn out to be very attractive. Simultaneously, it is worth to mention here the singular value decomposition as a potentially attractive algorithm which seems to be the most general and effective tool for solving this kind of problems. In the problem under consideration however, the direction of damage front propagation is easy to predict since it begins at the notch bottom and goes towards a symmetry axis, in other words along appropriate edge of finite element mesh. Above observation is a basis for application simplified technique in which subsequent boundary conditions are released following damage parameter D, reaching critical magnitude 0.9 in subsequent Gaussian points. Results of damage analysis done in such a way are shown in Fig. 4b. In subsequent hysteresis loops one can observe further difference in drop of stress amplitude between tension and compression as well as appearance of characteristic inflection point at hysteresis brunch referring to compressive range. This effect is strictly associated with contact of both edges of completely damaged element, next damage deactivation as a result of compression and consequently recovery of initial stiffness.

Table 2 Material constants of ferritic steel 20MnMoNi55

E [GPa]	ν	σ_{y} [MPa]	b	R_∞ [MPa]	X_∞ [MPa]	γ	S [MPa]
210	0.3	470	75	8.0	7500	70	5.0

4 Conclusions

Application of continuous damage deactivation gives both quantitative and qualitative good agreement with experimental data and confirms necessity and correctness of this approach in modelling of low cycle fatigue aluminum alloy Al-2024 and ferritic steel 20MnMoNi55.

Continuous damage deactivation concept applied to model of damage affected plastic potential recovers its convexity and smoothness, simultaneously allowing to avoid physically unjustified discontinuities.

References

1. Abdul-Latif, A., Chadli, M.: Modelling of the heterogeneous damage evolution at the granular scale in polycrystals under complex cyclic loadings. Int. J. Damage Mech. **16**(2), 133–158 (2007)
2. Brocks, W., Steglich, D.: Damage models for cyclic plasticity. In: Buchholtz, F.-G., Richard, H.A., Aliabadi, M.H. (eds) Advances in Fracture and Damage Mechanics. Trans Tech Publ, Zürich (2003)
3. Cegielski, M.: Effect of continuous damage deactivation in CDM. Ph.D. Thesis, Cracow University of Technology (2012)
4. Chaboche, J.-L.: Damage induced anisotropy: on the difficulties associated with the active/passive unilateral condition. Int. J. Damage Mech. **1**(2), 148–171 (1992)
5. Chaboche, J.-L.: Development of continuum damage mechanics for elastic solids sustaining anisotropic and unilateral damage. Int. J. Damage Mech. **2**, 311–329 (1993)
6. Chaboche, J.-L., et al.: Continuum damage mechanics, anisotropy and damage deactivation for brittle materials like concrete and ceramic composites. Int. J. Damage Mech. **4**, 5–21 (1995)
7. Cegielski, M., Ganczarski, A.: Effect of continuous damage deactivation on yield and failure surfaces. Acta Mech. Automatica **1**(2), 11–14 (2007)
8. Ganczarski, A., Cegielski, M.: Application of the continuous damage deactivation to a modelling of low cycle fatigue of aluminum alloy Al-2024. Czas Tech. **5**(105), 61–70 (2008)
9. Halm, D., Dragon, A.: A model of anisotropic damage by mesocrack growth; unilateral effect. Int. J. Damage Mech. **5**, 384–402 (1996)
10. Halm, D., Dragon, A.: An anisotropic model of damage and frictional sliding for brittle materials. Eur. J. Mech. A. Solids **17**(3), 439–460 (1998)
11. Hansen, N.R., Schreyer, H.L.: Damage deactivation. Trans. ASME **62**, 450–458 (1995)
12. Hayakawa, K., Murakami, S.: Thermodynamical modelling of elastic-plastic damage and experimental validation of damage potential. Int. J. Damage Mech. **6**, 333–363 (1997)
13. Ju, J.W.: On energy based coupled elastoplastic damage theories: constitutive modelling and computational aspects. Int. J. Solids Struct. **25**(7), 803–833 (1989)
14. Krajcinovic, D.: Damage mechanics. Elsevier, Amsterdam (1996)
15. Krajcinovic, D., Fonseka, G.U.: The continuous damage theory of brittle materials, part I and II. J. Appl. Mech. ASME **18**, 809–824 (1981)
16. Ladeveze, P., Lemaitre, J.: Damage effective stress in quasi-unilateral conditions. Proc IUTAM Congr Lyngby, Denmark (1984)
17. Lemaitre, J.: A course on damage mechanics. Springer, Berlin (1992)
18. Lemaitre, J., Chaboche, J.-L.: Mécanique des matériaux solides. Bordas, Paris (1985)
19. Litewka, A.: Creep damage and creep rupture of metals. Wyd Polit Poznańskiej (1991)
20. Mazars, J.: A model of unilateral elastic damageable material and its application to concrete. In: Wittmann, F.H. (ed) Energy Toughness and Fracture Energy of Concrete. Elsevier, Amsterdam (1986)

21. Murakami, S., Kamiya, K.: Constitutive and damage evolution equations of elastic-brittle materials based on irreversible thermodynamics. Int. J. Solids Struc. **39**(4), 473–486 (1997)
22. Ramtani, S.: Contribution á la modelisation du comportement multiaxial du beton endommagé avec description du caractere unilateral. Ph.D. Thesis, Univ Paris VI (1990)
23. Skrzypek, J.J., Ganczarski, A.: Modelling of material damage and failure of structures. Springer, Berlin (1999)
24. Skrzypek, J.J., Kuna-Ciskał, H.: Anisotropic elastic-brittle-damage and fracture models based on irreversible thermodynamic. In: Skrzypek, J.J., Ganczarski, A. (eds) Anisotropic Behaviour of Damaged Materials. Springer, Berlin (2003)